PROCEEDINGS B

royalsocietypublishing.org/journal/rspb

Research

Cite this article: Ezray BD, Wham DC, Hill CE, Hines HM. 2019 Unsupervised machine learning reveals mimicry complexes in bumblebees occur along a perceptual continuum. *Proc. R. Soc. B* **286**: 20191501. http://dx.doi.org/10.1098/rspb.2019.1501

Received: 29 June 2019
Accepted: 19 August 2019

Subject Category:
Evolution

Subject Areas:
evolution, ecology

Keywords:
Müllerian mimicry, *Bombus*, biogeography, coloration, convolutional neural network, machine learning

Author for correspondence:
Heather M. Hines
e-mail: hmh19@psu.edu

Electronic supplementary material is available online at https://doi.org/10.6084/m9.figshare.c.4643036.

THE ROYAL SOCIETY PUBLISHING

Unsupervised machine learning reveals mimicry complexes in bumblebees occur along a perceptual continuum

Briana D. Ezray[1], Drew C. Wham[2], Carrie E. Hill[2] and Heather M. Hines[1,2]

[1]Department of Entomology, and [2]Department of Biology, The Pennsylvania State University, University Park, PA 16802, USA

BDE, 0000-0002-9240-8606; DCW, 0000-0002-1946-9015; HMH, 0000-0003-0299-5569

Müllerian mimicry theory states that frequency-dependent selection should favour geographical convergence of harmful species onto a shared colour pattern. As such, mimetic patterns are commonly circumscribed into discrete mimicry complexes, each containing a predominant phenotype. Outside a few examples in butterflies, the location of transition zones between mimicry complexes and the factors driving mimicry zones has rarely been examined. To infer the patterns and processes of Müllerian mimicry, we integrate large-scale data on the geographical distribution of colour patterns of social bumblebees across the contiguous United States and use these to quantify colour pattern mimicry using an innovative, unsupervised machine-learning approach based on computer vision. Our data suggest that bumblebees exhibit geographically clustered, but sometimes imperfect colour patterns, and that mimicry patterns gradually transition spatially rather than exhibit discrete boundaries. Additionally, examination of colour pattern transition zones of three comimicking, polymorphic species, where active selection is driving phenotype frequencies, revealed that their transition zones differ in location within a broad region of poor mimicry. Potential factors influencing mimicry transition zone dynamics are discussed.

1. Background

Mimicry has long served as an example of evolution in action, with the exceptional diversity and convergence it generates informing both microevolutionary and macroevolutionary processes [1,2]. While defensive mimicry can involve palatable species mimicking unpalatable ones (i.e. Batesian mimicry), in Müllerian mimicry, harmful, sympatric species mimic each other by converging on a shared warning signal [3]. Müllerian mimicry phenotypes, often colour patterns, are generated and sustained through frequency-dependent selection driven by predator experience: predators learn to avoid colour patterns of harmful species they have previously sampled, leading to increased survival of species portraying the most abundant colour pattern [4–7].

It has been posited that frequency-dependent selection on a noxious lineage should promote a single, global warning colour pattern [2]. However, in nature, Müllerian mimicry systems display a global mosaic, whereby predominant mimetic patterns differ by geographical region [2,8–11]. Such patchworks of mimetic patterns are common across Müllerian mimicry systems, with examples in the unpalatable neotropical butterflies (e.g. *Heliconius* butterflies) [2,12], stinging velvet ants [13,14], toxin-secreting millipedes [10] and poison frogs [9].

Frequency-dependent selection is argued to drive these mimicry complexes to be fairly discrete with narrow, maladaptive transition zones between them [15]. Within a mimicry complex, Müllerian mimics are thought to display near-perfect resemblance as predators will exert strong selection pressure against imperfect mimics [4,16,17]. Examining features of mimicry complexes, including mimetic fidelity and transition zone characteristics, such as width

[18–20], location and ability to generate novel mimetic forms [21], can inform the selective processes leading to mimicry complex formation and maintenance. The shifting balance theory argues, for example, that the location of these zones may lie in hotspots of species turnover, such as climatic transition zones or contact zones between historic refugia, and that partial barriers to gene flow and low population sizes in these zones may promote shifts in mimicry pattern frequencies [22].

Bumblebees (Apidae: genus *Bombus* Latrielle) are a particularly well-suited system to study the factors driving defensive mimicry. They display exceptionally diverse segmental colour patterning across their Holarctic range, with 427 different colour patterns across the approximately 250 species [23,24], a diversity explained in part by convergence and divergence onto numerous Müllerian mimicry complexes [23]. The bright, warning colour patterns of these stinging bees have been demonstrated to be effective for predator avoidance [25,26], and geographical analysis across species revealed that their colour patterns cluster into at least 24 distinct mimicry complexes globally [23]. Mimicry also explains the exceptional polymorphism, as species that span multiple mimicry complexes tend to converge onto different mimicry patterns across their range (e.g. [11]). While examination of colour patterns at a coarse scale has been effective in defining mimicry complexes in bumblebees [23], understanding how they have evolved and are maintained requires a quantitative analysis at a fine spatial scale [8].

In this study, we seek to gain a better understanding of how mimicry complexes evolve by examining the extent of mimetic fidelity and the properties of mimicry transition zones in bumblebees across the United States at a fine scale. More specifically, we examine whether bumblebee colour patterns exhibit mimicry, whether bumblebee mimicry tends to be perfect or imperfect, and whether mimicry transition zones are discrete, with narrow transition zones, as has been found in butterflies [2]. This is accomplished by using the extensive database of bumblebee distributional records on Global Biodiversity Information Facility (GBIF) (approx. 1 in 200 current GBIF records is a bumblebee) and detailed documentation of their respective colour patterns. To quantify mimetic fidelity with minimal *a priori* bias, we use a novel machine-learning-based method to calculate perceptual distance between colour patterns [27]. Finally, to better understand factors actively driving mimicry dynamics, we compare transition zone characteristics and the potential role of climate in driving the distribution of three polymorphic species, *Bombus flavifrons*, *B. melanopygus* and *B. bifarius*, that shift between the Pacific Coastal and Rocky Mountain mimicry patterns by changing their abdominal segments from black to ferruginous (rust-coloured), thus undergoing mimetic changes in parallel.

2. Material and methods

(a) Characterizing general mimicry patterns

(i) Mimetic fidelity of bumblebee colour patterns

To assess the similarity between bumblebee colour patterns, we used a standardized template. A template removes effects of body size while still maintaining the 'morphologically monotonous' shape of bumblebees [28], allowing us to focus only on colour pattern differences and avoid inaccuracies from differing perspectives, light conditions or sizes. The template used for building our colour diagrams was drawn with consideration of proportional sizes of each body segment (see electronic supplementary material, figure S1). Colour diagrams were built for all bumblebee species occurring in the contiguous United States, excluding the rare and highly colour-pattern-variable parasitic bumblebees (*Psithyrus*), by applying particular colours to each segmental domain of our template to match the colour patterns displayed in [29]. In total, this included 35 bumblebee species with 64 worker patterns (queens exhibit identical or similar patterns) (e.g. see electronic supplementary material, figure S2). Colours, including yellow, black, brown, white, ferruginous or yellow-black (olive) (see electronic supplementary material, figure S1), were equivalent to the colour classes used in [23] and were applied to the template using Adobe Illustrator CC (2018). Thus far, all bumblebee species have been observed to use the same pigments for each respective colour [30,31], therefore the UV reflectance of each colour should be conserved across species and only saturation is likely to differ substantially. As saturation can be variable intraspecifically and has not been previously quantified, we focus here on colour pattern differences, rather than minor variations in colour. Templates were exported at 256×256 pixel resolution for analyses.

An innovative machine-learning approach was used to quantify perceptual similarity among bumblebee colour patterns [27]. This method uses a deep convolutional neural network (AlexNet) [32] previously trained for large-scale image recognition. During the training process, this neural network learned visual 'features' including fine-scale edges, textures and colour contrasts, from 1.2 million images including diverse inanimate and animate objects at a variety of scales [32]. After the training process, when a new image is passed through the network, the output is a numerical representation of the detection (activation) of each of the learned features. These activations create a numerical vector representation of the image. A perceptual distance metric can then be generated based on the distance between the vectors of two images [33]. This perceptual distance metric has been demonstrated to closely match human judgement and significantly outperforms some of the most commonly used techniques for quantifying perceptual distance [33]. This method thus provides a reliable, data-rich metric for the quantification of mimicry dynamics that, in contrast to other quantitative pixel-based approaches [23,34], is not overly sensitive to slight shifts in the location of pattern elements [27].

Following the methods proposed by Wham *et al*. [27], we used this approach to calculate the perceptual distance between every pairwise set of bumblebee colour pattern diagrams. We then performed t-distributed stochastic neighbour embedding (t-SNE) [35,36], a common technique for visualizing high dimensionality distances in a two-dimensional plot. Bumblebee templates were plotted at their corresponding x, y coordinate position, avoiding overplotting. Perceptual distances between the colour patterns are used as a metric of mimetic fidelity with patterns closer together representing better mimics. To visualize spatial positioning from the t-SNE plot, a colour wheel was arbitrarily applied to the t-SNE plot (electronic supplementary material, figure S3). The relative location of each x, y coordinate could then be represented graphically with a single colour (embedded colour code) and the distances between x, y coordinates of colour patterns thus visualized by relative differences in colour on the colour wheel. Scripts for this analysis are available at https://github.com/DrewWham/Perceptual_tSNE.

(ii) Distributional analysis of bumblebee colour patterns

To analyse geographical distributions of colour patterns, we assigned colour patterns to specimen data extracted from GBIF.

We downloaded preserved specimen data for all social bumblebees found in the contiguous United States, representing a total of 160 213 records from 35 species (electronic supplementary material, figure S2) [37]. Data were assessed for accuracy based on accepted distributions of species ranges (cf. [29]) and specimens with localities falling well outside the documented range were removed. We confirmed this dataset to be robust for assessing relative abundance of species at a scale of 900 cells across the United States (cell size of 167 km × 88 km) by examining raster maps of specimen abundance and species richness in R using raster [38], maps [39] and ggplot2 [40].

To determine how colour patterns cluster geographically, we created raster maps (900 grid cells; approx. 167 km × 88 km) depicting estimates of the average perceptual colour patterns of bumblebee species across the United States. For this, we calculated the perceptual mimicry optimum by averaging colour patterns among all specimens contained in a grid cell (perceptual colour pattern frequency). We also calculated the average colour pattern across species morphs present in a grid cell, considering each species morph only once (colour pattern average). This metric assesses convergence of colour patterns among species (species mimicry) as relative abundances of individuals within a species are not considered. Averages for each grid cell were calculated from the x, y coordinate values of colour patterns from the t-SNE analysis. For monomorphic species, we assigned all specimens of the species the same colour pattern x, y coordinate values. For polymorphic species, we assigned colour pattern x, y coordinate values to locality data based on the literature (electronic supplementary material, figure S4). Grid cells containing fewer than 10 specimens (perceptual colour pattern frequency) and less than two unique colour patterns (colour pattern average) were removed from the analysis. Spatial analyses were performed in R using raster [38] and BBmisc [41]. To estimate the number of mimetic clusters occurring geographically, the average x, y coordinate values were extracted from each grid cell of the raster maps and the optimal number of clusters were estimated in R using the ClusterR package [42] by applying Optimal K means analyses and examining the Bayesian information criterion (BIC).

To determine if specific, abundant species influence perceptual colour pattern frequencies, we used ArcGIS 10.3 to determine the most frequent species from GBIF data in each region (resolution: cell size approx. 142 km^2; 663 cells total). Finally, a raster map of perceptual colour pattern variance (the spread compared to the mean of x, y coordinates of colour patterns) in 900 cells across the United States (cell size: 167 km × 88 km) was created in R using raster [38], maps [39] and ggplot2 [40].

(iii) Assessing convergence in warning signals

An important element of mimicry is that the sympatric phenotypes are convergent [43]; however, previous analyses did not consider phylogeny in assessing the degree of mimicry in bumblebee species [23]. To examine the degree of convergence and how colour patterns have evolved, we created a dendrogram of perceptual colour pattern distances, as calculated by the convolutional neural network, using the R program ape [44] and dendextend [45]. Perceptual colour pattern distances were compared to distances of the bumblebee phylogenetic tree [30], including each species found in the contiguous United States, using a Mantel test [46] (R program ade4 [47], 9999 matrix permutations). To visualize the phylogenetic and perceptual colour pattern relationships, we assigned the species-specific embedded colour code to the branches of the bumblebee phylogenetic tree (electronic supplementary material, figure S5) and the dendrogram of perceptual colour pattern distances (figure 1*b*).

(b) Mimetic transition zone dynamics in polymorphic species

(i) Mimetic distribution and fidelity

We analysed the fine-scale distribution of colour pattern variability within three polymorphic species, *B. flavifrons*, *B. melanopygus* and *B. bifarius*, using detailed phenotypic data collected from approximately 300 newly collected individuals and 4921 museum specimens (*B. flavifrons*: 268; *B. melanopygus*: 2663; *B. bifarius*: 1990), from seven natural history museums. Specimens included queens, workers and drones (males). For each individual, colour percentages (black, ferruginous, yellow, brown or white) were assigned to each section of the body, including 72 regions for females (queens and workers) and 88 for males (electronic supplementary material, figure S6), similar to [24]. Specimen identifications were checked, and deemed mostly correct, attesting to the accuracy of identifications in museum collections. From these data, we made distributional maps (R: ggplot2 [40], ggthemes [48]) using georeferenced locality data of the colour pattern variation most relevant to mimicry, plotting overall percentage of black versus ferruginous colour in metasomal tergites 2 and 3 for *B. melanopygus* and *B. bifarius* (electronic supplementary material, figure S7), and tergite 3 in *B. flavifrons*.

To understand how mimetic fidelity varies across these species' ranges, we assessed the degree to which the colour patterns of each polymorphic species differed from the local perceptual colour pattern frequency. For each specimen, we calculated Euclidian distance between the t-SNE x, y coordinates for its colour pattern and the perceptual colour pattern frequency for all bumblebees located in the grid cell where the specimen occurred. Distances across all specimens in a grid cell were averaged for each species and plotted geographically. Scripts for spatial and evolutionary analyses are available on GitHub: https://github.com/bdezray/Bumble-bee-Color-Mimicry.

(ii) Potential forces driving distributions

To examine whether mimetic transition zones in these polymorphic bumblebees occur in climatic transition zones, we performed ecological niche modelling to predict the distribution of each colour pattern based on climatic preferences. If the localities for one colour pattern predict a niche distribution that encompasses the range of the other colour pattern, that would suggest they both occupy similar climatic zones. Additionally, we removed localities located in the transition zone and inferred whether climatic models alone could predict the range of each colour pattern within the transition zone. Niche modelling was performed in MaxEnt [49] using raster layers for 19 WorldClim bioclimatic variables that account for temperature and precipitation at yearly, quarterly, and monthly time scales (1950–2000 climate, 30 s resolution [50]) (electronic supplementary material, table S1). Each raster layer was clipped to the study extent and converted to an ASCII file in R using the package raster [38] and run through 15 cross-validated replicates, with model performance assessed using the AUC statistic. The output was visualized in QGIS3 [51].

3. Results

(a) Mimetic fidelity among bumblebees in the United States

Our analysis of the similarities among bumblebee colour patterns displayed in figure 1*a* shows that bumblebees that are traditionally assigned to the same mimicry zones and geographical regions tend to be closer to each other. However, bumblebee colour patterns do not form discrete clusters of

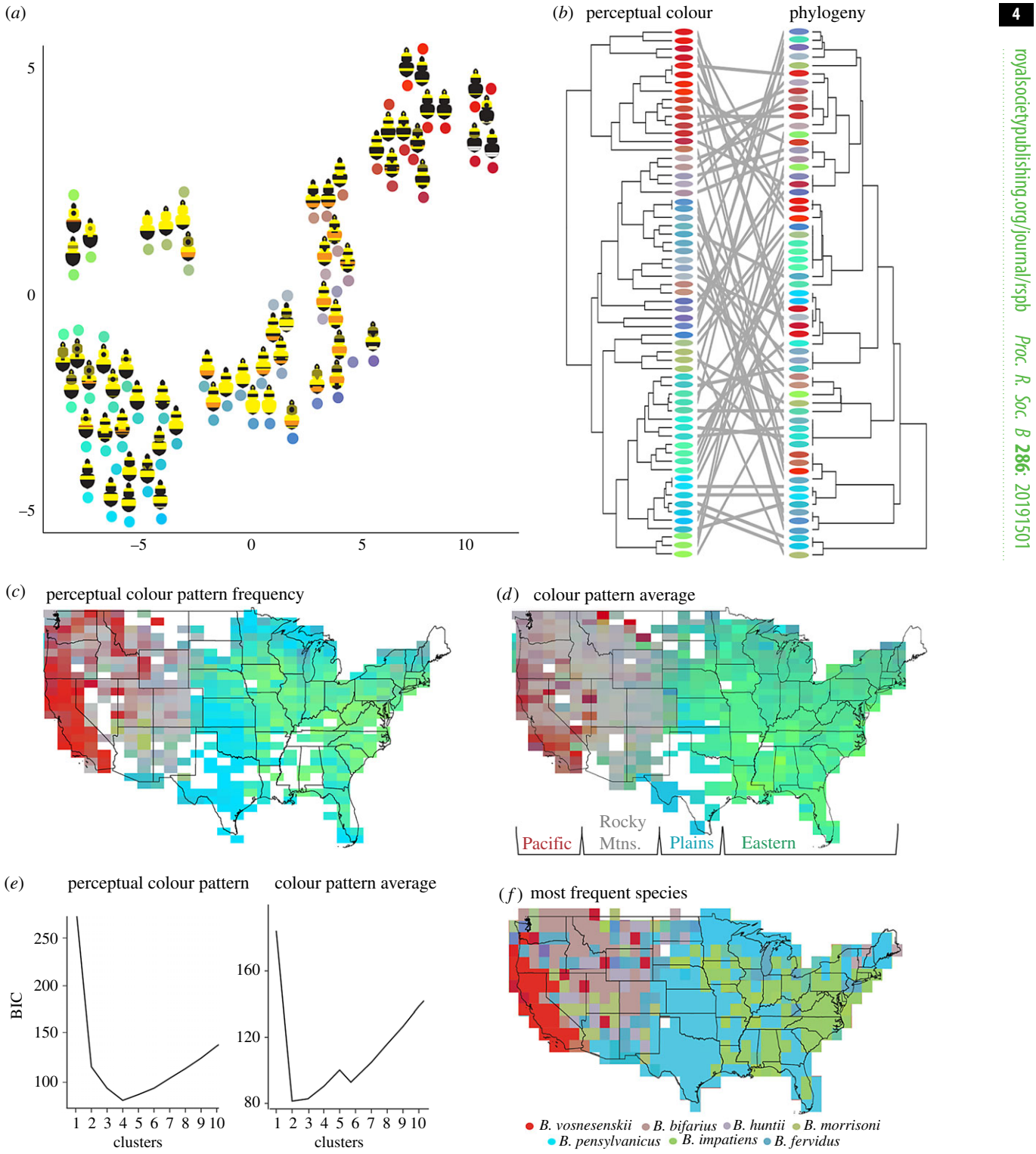

Figure 1. Quantification of mimetic patterns among bumblebees of the USA. (*a*) t-SNE plot of perceptual colour pattern embedding values. (*b*) Topology of colour pattern similarity (left) compared with phylogenetic history [30] (right) with embedding colour code for each taxon and tanglegram lines connecting the same taxon. (*c*) Fine-scale depiction of perceptual colour pattern frequencies calculated by averaging t-SNE positions of all bumblebee specimens contained within each grid cell. (*d*) Average colour embedded score by species/colour form. (*e*) Optimal number of clusters occurring geographically for the perceptual colour pattern frequency and the colour pattern average. The optimal number of clusters occurs when the Bayesian information criterion (BIC) is lowest. (*f*) The most frequent species coloured by the embedding colour codes. These species include *B. vosnesenskii* (red), *B. bifarius* (grey), *B. huntii* (light purple), *B. morrisoni* (pale green), *B. pensylvanicus* (blue), *B. impatiens* (green) and *B. fervidus* (teal).

similar colour patterns as one might expect with mimicry systems, but rather fall on a continuum of perceptual variation (figure 1*a*). We see a gradual shift in colour patterns from the bottom left corner to the top right corner of figure 1*a*, which reflects the transition from eastern to western colour patterns across the United States.

(b) Spatial distribution of mimicry complexes

Ample specimen data is available across grid cells throughout most of the United States (median abundance per grid cell = 74), making the GBIF data a meaningful representation of communities at this spatial scale (electronic supplementary material, figure S8). Species richness is greatest within the

Rocky Mountain region and along the Pacific Coast, matching expectations from natural species richness, suggesting species diversity is captured well (electronic supplementary material, figure S8). The lowest specimen abundance and species richness occurs in the Great Plains and southern USA (electronic supplementary material, figure S8). While this represents natural abundance in the Southwest, parts of the Southeast and Great Plains are likely to be undersampled.

From our analysis comparing the perceptual colour pattern frequency for every grid cell within the United States, it is clear that the colour patterns of bumblebees differ by geographical region. Our raster plot (figure 1*c*) and cluster analysis (figure 1*e*) support four major colour pattern complexes, including Pacific Coastal, Rocky Mountain, Great Plains and Eastern mimicry regions. In our analysis of colour pattern averages, where we assess if comimicry is occurring, the same clusters are visually apparent to some degree (figure 1*d*), but two to three clusters are statistically favoured (figure 1*e*), as Pacific Coastal and Great Plains mimicry complexes are reduced in range (figure 1*d*). Such a reduction is particularly apparent when examining the colour pattern average in northern California and Oregon where colour pattern diversity exists, as neighbouring grid cells show more variation (figure 1*d*) and there is higher variance within grid cells (electronic supplementary material, figure S8). Based on the observed most frequent species, in the Pacific Coastal and the Great Plains mimicry complexes, it is likely that the dominant species, *B. vosnesenskii* and *B. pensylvanicus*, respectively, are driving the perceptual colour pattern frequency (figure 1*f*).

(c) Evolution of shared warning signals

In examining bumblebee colour patterns within the United States mapped onto the phylogeny, it is apparent that similar colour patterns are scattered across distant lineages. In addition, there was no significant correlation between phylogenetic and perceptual colour pattern distance ($r = 0.0701$, $p = 0.1051$) (figure 1*b*).

(d) Mimetic transition zones in polymorphic species

The *B. flavifrons* transition zone aligns fairly well with the Pacific Coastal–Rocky Mountain transition zone (figures 2*a* and 1*c*). *B. flavifrons* appears to exhibit relatively good mimetic fidelity outside the colour pattern transition zone, but, apart from the intermediate form, is a poor mimic within the transition zone (figure 2*b*). The primary *B. melanopygus* hybrid zone is located west of the typical hybrid zone of all species (figures 2*e* and 1*c*). The ferruginous and black forms are good mimics where these forms typically occur (figures 2*f* and 1*c*), but where there are no other abundant, ferruginous species, in the Pacific Northwest to northern California, this pattern is a poor mimic (figure 2*f*). In *B. bifarius*, the inferred hybrid zone is eastern shifted relative to the other polymorphic species (figure 2*i*) and the Pacific Coastal–Rocky Mountain hybrid zone (figure 1*c*), with this zone transitioning from black to ferruginous with a continuum of intermediate colour patterns (figure 2*i*). The fidelity of the black, ferruginous and intermediate forms each varies with the highest fidelity observed on the far western and eastern extents of this species range. It is especially apparent that the black form is shifted further east than is optimal in the eastern portion of its range and the intermediate form sustains decent fidelity throughout its distribution suggesting that it may garner protection in both predominately black and ferruginous populations (figure 2*j*).

Niche models fail to predict that colour patterns occur within each other's range for all three polymorphic species (figure 2*c*,*g*,*k*), suggesting climatic differences between the regions of each form. When localities from each respective hybrid zone are removed, climate somewhat predicts the ferruginous colour morph distribution of each species. However, it does not predict the range of the black form, suggesting that the black forms occupy a more distinct climatic region and that each species extends beyond this climatic optimum for this form (figure 2*d*,*h*,*l*).

4. Discussion

Müllerian mimicry systems exhibit extraordinary diversity of colour patterns due to their colour pattern convergence within and divergence between mimicry complexes, making them model systems for understanding how phenotypes evolve. While several studies have examined the distributions of these mimetic forms in a broad sense [10,13,23], the finer-scale analysis needed to better reveal how mimicry complexes form and are maintained [8] has been limited by access to high-resolution data. The exceptional distributional and colour pattern data of bumblebees enable such fine-scale analyses.

Quantifying colour pattern similarity has also been a major challenge for detailed analysis of mimetic fidelity as it requires a reliable metric for quantification. Previous approaches analysing colour pattern similarity by pixel [23,34] are overly sensitive to slight shifts in the location of pattern elements that may have little impact on pattern recognition by predators [23,52]. Coding systems that recognize relative locations of pattern elements, such as colours and contrasts [13,23], can be subjective, lack consideration of relative sizes/shape and involve a limited number of characters. Ranks of similarity from human observers [13,53] provide metrics of mimetic fidelity, but can be sensitive to survey design. The machine-learning approach used here has been demonstrated to be robust to these challenges, allowing unsupervised analysis of continuous colour pattern variability [27]. This approach is therefore ideal for scoring perceptual colour pattern differences, enabling the quantification of mimetic fidelity on a continuous scale.

The machine-learning approach applied here is based on human perception, rather than a particular predators' perceptual model [54] (e.g. optimized for colour vision extending into the UV spectrum or differences in visual acuity); however, we suggest that a generalized perceptual model might be desirable. The predators of foraging bumblebees in temperate regions span from other arthropods, such as robber flies [55,56] and spiders [57,58], to birds [59,60], as well as amphibians and reptiles [61,62]. Bumblebees therefore have numerous predators with variable visual models. Additionally, differences in UV which would not be accounted for in human perceptual models are not expected either within or between bumblebee species as their colours involve the same pigments [30,31]. In this context, we propose that a perceptual model based on computer vision and human perception can provide a reasonable metric of mimetic fidelity.

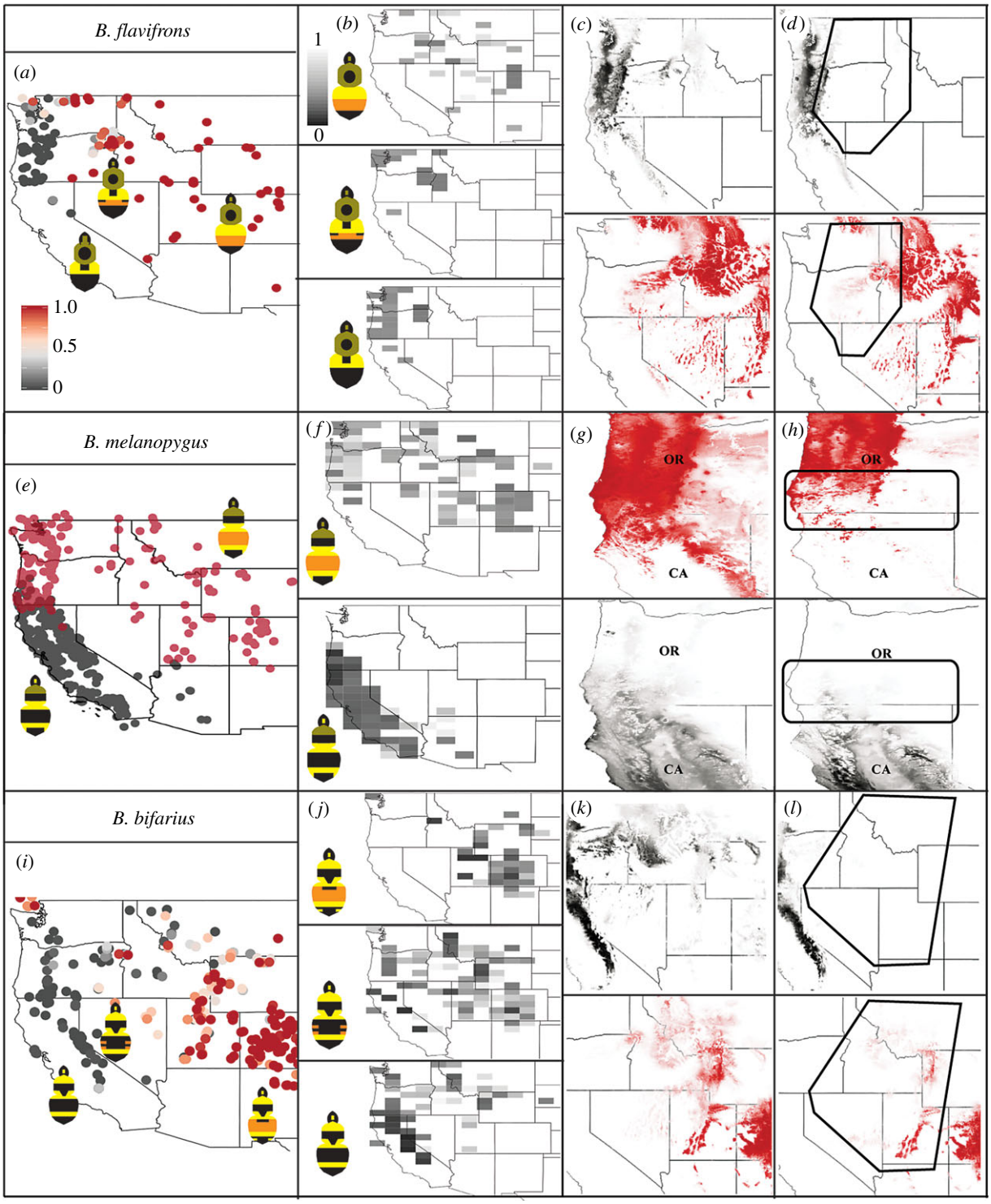

Figure 2. Mimetic transition zone dynamics in three polymorphic species. The left panel shows locality maps of colour pattern transition zones and distributions for (*a*) *B. flavifrons*, (*e*) *B. melanopygus* and (*i*) *B. bifarius*. The scale bar represents the percentage of ferruginous for *B. flavifrons* and *B. bifarius*, which exhibit continuous variation. (*b*,*f*,*j*) Regional mimetic fidelity of colour patterns of each species, with darker colours indicating a better match to the perceptual colour pattern frequency and separate analyses run for all ferruginous, all black, and intermediate colour patterns. (*c*,*g*,*k*) The impact of climatic conditions on colour pattern distribution with niche models of full ferruginous and black colour pattern variants modelled separately, and (*d*,*h*,*l*) the same models with specimens from the hybrid zone (outlined regions) excluded.

(a) Müllerian mimicry complexes in bumblebees are continuous

Our analyses support mimicry in bumblebees: similar colour patterns cluster in distinct geographical zones (figure 1*c*) and are convergent, as they map to different places in the phylogeny (figure 1*b*). The geographical data and cluster analysis support the three mimicry complexes for US bumblebees (Pacific Coastal, Rocky Mountain and Eastern) previously recognized at a coarse-scale [23], as well as an additional Great Plains mimicry complex (figure 1*c*,*e*).

Mimicry theory states that frequency-dependent selection should pull species toward a shared colour pattern for each region [2,8], generating discrete mimicry complexes. Previous research examining the geographical clustering of similar colour patterns using a binning approach at a coarse geographical scale, ascribed bumblebees to multiple, discrete mimicry groups [23]. While we recognize these mimicry

groups, we found that when examined at a fine-scale these patterns are not discrete, as bumblebees exhibit a manifold of perceptual colour patterns (figure 1*a*). This colour pattern continuum reflects their geographical distribution from west to east, suggesting that colour patterns tend to transition more on a gradient across geographical space as opposed to occupying discrete groups (figure 1*a*,*c*).

In nature, mimicry is often imprecise [16]. Imperfect mimicry has previously been observed to occur when velvet ants in transitional zones adopt a single colour pattern that broadly matches two different mimicry complexes [63]. We also observe taxa displaying patterns in between traditional mimetic patterns (figure 1*a*,*c*) when they span mimicry complexes. For example, *B. mixtus* exhibits a single colour pattern across the Pacific Coastal and Rocky Mountain mimicry complexes. This pattern fits between colour pattern clusters (figure 1*a*; electronic supplementary material, figure S2), thus acting as an imperfect mimic of both regions. In the transition zone, an intermediate pattern may even be favoured, as it may best represent the perceptual colour pattern average. Additionally, it has previously been hypothesized that predators will resort to pattern generalization as colour pattern variance increases due to either limited memory capability [64] or risk aversion [65]. Our data show a broad region with poor mimicry in the Pacific Northwest where there is high variance and mimicry zones transition (electronic supplementary material, figure S8). In such cases, frequency-dependent selection would result in reduced directional selection favouring any given phenotype, thus allowing mimicry diversity and/or imperfect mimicry to persist [63,66,67].

Given that some mimicry zones with nearly identical patterns exist (e.g. Southern Rockies) (figure 1*d*), predators can probably discriminate and select for more perfect mimicry. However, selection dynamics can also be influenced by the predator community present, flight ranges of experienced birds in the transition zone, and the ease of detecting colour patterns by habitat. Furthermore, the more harmful a prey is the less likely predators will take risks, which could explain why more imperfect mimics are apparent in bumblebees and velvet ants [63] than in butterflies. Bumblebees, as social insects, may also generate protection from predator exposure to their own kin, which could decrease the strength of selection on precise mimicry of local forms [68,69].

(b) Colour transition zones inform the evolution of mimicry

Contact zones tend to be shared across organisms [70,71]. Our data support major transition zones in mimicry complexes occurring in recognized hotspots of faunal turnover. The eastern transition zone is a common faunal transition zone [71], including for bumblebees, which exhibit nearly complete species turnover along the eastern foothills of the Rocky Mountain range. The transition zone between the Pacific Coastal and Rocky Mountain mimicry complexes is between two major mountain chains and a desert, thus supporting the hypothesis that major barriers to dispersal and gene flow could drive the location of mimicry transition zones [43,71,72]. There is sharing of Pacific Coastal and Rocky Mountain fauna, although there are several species restricted in their distribution to the Pacific Coastal states, suggesting this transition zone naturally acts as a climatic or topographic barrier. The transition zone between the Pacific Coastal and Rocky Mountain mimicry complexes is a common hybrid zone in other organisms including birds, mammals and trees [71].

Our analysis examining the distribution of *B. flavifrons*, *B. melanopygus*, and *B. bifarius* colour patterns revealed that the locations of transitions zones differ between species. Most notably, the ferruginous morph of *B. melanopygus* and black morph of *B. bifarius* extend into regions where these patterns are suboptimal (figure 2*f*,*j*). The transition zone of *B. melanopygus* is located in a region where many other hybrid zones occur, recognized as a contact zone generated upon glacial recession [71]. A possible scenario, which adheres to the leading-edge hypothesis, is that a black form evolved in southern refugia to converge onto a local mimicry pattern and later came into secondary contact in its current location with the ferruginous form which was able to fill in the unoccupied space post glaciation more rapidly [73,74]. The location of intermediate patterns in *B. bifarius* falls in an area with less perfect mimicry (figure 1*c*,*d*) which could enable it to be a partial mimic of both Pacific Coastal and Rocky Mountain forms. Intermediate patterns could variably serve an advantage or be under weaker forces of selection. Furthermore, colour pattern inheritance dynamics, including genetic complexity and dominance, could hypothetically influence the location of mimicry transition zones. The ferruginous-black colour pattern variation observed in *B. melanopygus* (figure 2*e*; electronic supplementary material, figure S7) is controlled by a single Mendelian gene [75], whereas *B. bifarius* exhibits a gradation of intermediate colour patterns (figure 2*i*; electronic supplementary material, figure S7), suggesting multigenic regulation. The greater complexity in gene regulation in *B. bifarius* may result in the relatively wider hybrid zone in this species compared to the hybrid zone in *B. melanopygus*. Furthermore, the ferruginous morph is dominant over the black morph for *B. melanopygus*. Following the principle of dominance drive [76,77], the dominance of the ferruginous morph could impact the movement of the hybrid zone, driving the ferruginous form westward.

5. Conclusion

Bumblebee taxonomy has often relied on differences in colour patterns, resulting in the availability of remarkable documentation of colour pattern data. The abundance, importance, general charisma and ease of sight identification of these pollinators has also resulted in them being one of the most heavily georeferenced taxa. Using these data resources and a novel deep-learning-based metric of perception, our data support the geographical convergence of colour patterns among bumblebees. However, contrary to mimicry theory and traditional interpretation of mimicry complexes, our data suggest mimicry in bumblebees involves extensive continuous variation both in geographical and colour pattern space. This continuum may result from relaxed selection in mimetic transition zones that permit or even favour imperfect mimicry. In addition, we observed the locations of mimicry transition zones to differ among polymorphic species, which could be explained by relaxed selection in these zones, but also additional factors such as historical biogeography, climate, dominance drive and genetic complexity.

Through the use of an innovative, machine-learning approach to assess mimetic fidelity, we were able to quantify colour pattern fidelity in a way that is perhaps the most rigorous to date. This technique will expand opportunities to quantify mimicry towards many questions across mimicry systems, such as understanding the role of prey community richness and complexity, participation of numerous organisms across communities in mimicry complexes, and the evolution of mimicry patterns.

Data accessibility. The associated analysis files, climate data and MaxEnt input files reported in this paper have been deposited in the Dryad Digital Repository: https://doi.org/10.5061/dryad.sd7cd06. The scripts reported in this paper have been deposited in the following GitHub Repositories: (1) https://github.com/DrewWham/Perceptual_tSNE; (2) https://github.com/bdezray/Bumble-bee-Color-Mimicry.

Authors' contributions. B.D.E., D.C.W. and H.M.H. designed research; B.D.E., D.C.W., C.E.H., H.M.H. performed research; B.D.E., C.E.H. and H.M.H. assisted in specimen acquisition and processing; B.D.E. and H.M.H. curated data; B.D.E. and D.C.W. managed data repositories; B.D.E., D.C.W., H.M.H. analysed data; and B.D.E., D.C.W. and H.M.H. wrote the paper.

Competing interests. We declare we have no competing interests.

Funding. This work was supported by the NSF CAREER Grant DEB1453473 awarded to H.M.H.

Acknowledgements. We acknowledge Rebecca Sommer, Luca Franzini, Sarthok Rahman, Li Tian and Patrick Lhomme for their support in acquiring specimens. Thanks to Li Tian for images of *B. melanopgyus* and *B. bifarius*. We thank the AMNH, Smithsonian Museum of Natural History, Peabody Museum of Natural History, Essig Museum, Bohart Museum, Oregon State Arthropod Collection and the USDA Systematics and Biology Laboratory at Utah State University (U.S. National Pollinating Insect Database) for providing specimen to phenotype. Thanks to Sydney Cameron, Jamie Strange and Jeffrey Lozier for initial discussions. We thank Margarita Lopez-Uribe, Christina Grozinger, Erica Smithwick, Diana Cox-Foster, Elyse McCormick and reviewers for helpful comments on the manuscript.

References

1. Quicke DL. 2017 *Mimicry, crypsis, masquerade and other adaptive resemblances*. Hoboken, NJ: Wiley Blackwell.
2. Mallet J, Joron M. 1999 Evolution of diversity in warning colour and mimicry: polymorphisms, shifting balance, and speciation. *Annu. Rev. Ecol. Syst.* **30**, 201–233. (doi:10.1146/annurev.ecolsys.30.1.201)
3. Müller F. 1879 Ituna and Thyridia: a remarkable case of mimicry in butterflies. *Trans. Entomol. Soc. Lond.* **1879**, 20–29.
4. Ruxton GD, Sherratt TN, Speed MP, Speed MP, Speed M. 2004 *Avoiding attack: the evolutionary ecology of crypsis, warning signals and mimicry*. Oxford, UK: Oxford University Press.
5. Kapan DD. 2001 Three-butterfly system provides a field test of Müllerian mimicry. *Nature* **409**, 338–340. (doi:10.1038/35053066)
6. Joron M, Iwasa Y. 2005 The evolution of a Müllerian mimic in a spatially distributed community. *J. Theor. Biol.* **237**, 87–103. (doi:10.1016/j.jtbi.2005.04.005)
7. Chouteau M, Angers B. 2011 The role of predators in maintaining the geographic organization of aposematic signals. *Am. Nat.* **178**, 810–817. (doi:10.1086/662667)
8. Sherratt TN. 2006 Spatial mosaic formation through frequency-dependent selection in Müllerian mimicry complexes. *J. Theor. Biol.* **240**, 165–174. (doi:10.1016/j.jtbi.2005.09.017)
9. Symula R, Schulte R, Summers K. 2001 Molecular phylogenetic evidence for a mimetic radiation in Peruvian poison frogs supports a Müllerian mimicry hypothesis. *Proc. R. Soc. Lond. B* **268**, 2415–2421. (doi:10.1098/rspb.2001.1812)
10. Marek PE, Bond JE. 2009 A Müllerian mimicry ring in Appalachian millipedes. *Proc. Natl Acad. Sci. USA* **106**, 9755–9760. (doi:10.1073/pnas.0810408106)
11. Hines HM, Williams PH. 2012 Mimetic colour pattern evolution in the highly polymorphic *Bombus trifasciatus* (Hymenoptera: Apidae) species complex and its comimics. *Zoolog. J. Linnean Soc.* **166**, 805–826. (doi:10.1111/j.1096-3642.2012.00861.x)
12. Sheppard PM, Turner JRG, Brown KS, Benson WW, Singer MC. 1985 Genetics and the evolution of Muellerian mimicry in *Heliconius* butterflies. *Phil. Trans. R. Soc. Lond. B***308**, 433–610. (doi:10.1098/rstb.1985.0066)
13. Wilson JS, Williams KA, Forister ML, Von Dohlen CD, Pitts JP. 2012 Repeated evolution in overlapping mimicry rings among North American velvet ants. *Nat. Commun.* **3**, ncomms2275. (doi:10.1038/ncomms2275)
14. Wilson JS, Jahner JP, Forister ML, Sheehan ES, Williams KA, Pitts JP. 2015 North American velvet ants form one of the world's largest known Müllerian mimicry complexes. *Curr. Biol.* **25**, R704–R706. (doi:10.1016/j.cub.2015.06.053)
15. Mallet J. 1993 Speciation, raciation, and colour pattern evolution in *Heliconius* butterflies: evidence from hybrid zones. In *Hybrid Zones Evol. Process* (ed. RG Harrison), pp. 226–260. New York, NY: Oxford University Press.
16. Sherratt TN. 2002 The evolution of imperfect mimicry. *Behav. Ecol.* **13**, 821–826. (doi:10.1093/beheco/13.6.821)
17. Penney HD, Hassall C, Skevington JH, Abbott KR, Sherratt TN. 2012 A comparative analysis of the evolution of imperfect mimicry. *Nature* **483**, 461–464. (doi:10.1038/nature10961)
18. Mallet J, Barton N, Lamas G, Santisteban J, Muedas M, Eeley H. 1990 Estimates of selection and gene flow from measures of cline width and linkage disequilibrium in heliconius hybrid zones. *Genetics* **124**, 921–936.
19. Dasmahapatra KK, Blum MJ, Aiello A, Hackwell S, Davies N, Bermingham EP, Mallet J. 2002 Inferences from a rapidly moving hybrid zone. *Evolution* **56**, 741–753. (doi:10.1111/j.0014-3820.2002.tb01385.x)
20. Owen RE. 1986 Gene frequency clines at X-linked or haplodiploid loci. *Heredity* **57**, 209–219. (doi:10.1038/hdy.1986.111)
21. Jiggins CD, Mallet J. 2000 Bimodal hybrid zones and speciation. *Trends Ecol. Evol.* **15**, 250–255. (doi:10.1016/S0169-5347(00)01873-5)
22. Mallet J. 2010 Shift happens! Shifting balance and the evolution of diversity in warning colour and mimicry. *Ecol. Entomol.* **35**, 90–104. (doi:10.1111/j.1365-2311.2009.01137.x)
23. Williams P. 2007 The distribution of bumblebee colour patterns worldwide: possible significance for thermoregulation, crypsis, and warning mimicry. *Biol. J. Linnean Soc.* **92**, 97–118. (doi:10.1111/j.1095-8312.2007.00878.x)
24. Rapti Z, Duennes MA, Cameron SA. 2014 Defining the colour pattern phenotype in bumble bees (*Bombus*): a new model for evo devo. *Biol. J. Linnean Soc.* **113**, 384–404. (doi:10.1111/bij.12356)
25. Brower LP, Brower JVZ, Westcott PW. 1960 Experimental studies of mimicry. 5. The reactions of toads (*Bufo terrestris*) to bumblebees (*Bombus americanorum*) and their robberfly mimics (*Mallophora bomboides*), with a discussion of aggressive mimicry. *Am. Nat.* **94**, 343–355. (doi:10.1086/282137)
26. Evans DL, Waldbauer GP. 1982 Behavior of adult and naive birds when presented with a bumblebee and its mimic. *Ethology* **59**, 247–259. (doi:10.1111/j.1439-0310.1982.tb00341.x)
27. Wham DC, Ezray BE, Hines HM. 2019 Measuring perceptual distance of organismal color pattern using the features of deep neural networks. *bioRxiv*. (doi:10.1101/736306)
28. Michener CD. 1990 Classification of the Apidae (Hymenoptera). *Univ. Kansas Sci. Bull.* **54**, 75–164.
29. Williams PH, Thorp RW, Richardson LL, Colla SR. 2014 *Bumble bees of North America: an identification guide*. Princeton, NJ: Princeton University Press.

30. Hines HM. 2008 *Bumble bees (Apidae: Bombus) through the ages: historical biogeography and the evolution of colour diversity*. Urbana IL: University of Illinois at Urbana-Champaign.
31. Hines HM, Witkowski P, Wilson JS, Wakamatsu K. 2017 Melanic variation underlies aposematic color variation in two hymenopteran mimicry systems. *PLoS ONE* **12**, e0182135. (doi:10.1371/journal.pone.0182135)
32. Krizhevsky A, Sutskever I, Hinton GE. 2012 Imagenet classification with deep convolutional neural networks. In *Advances in neural information processing systems*, pp. 1097–1105.
33. Zhang R, Isola P, Efros AA, Shechtman E, Wang O. 2018 The unreasonable effectiveness of deep features as a perceptual metric. *arXiv preprint*.
34. Dittrigh W, Gilbert F, Green P, McGregor P, Grewcock D. 1993 Imperfect mimicry: a pigeon's perspective. *Proc. R. Soc. Lond. B* **251**, 195–200. (doi:10.1098/rspb.1993.0029)
35. Van Der Maaten L, Hinton G. 2008 Visualizing data using t-SNE. *J. Mach. Learn. Res.* **9**, 2579–2605.
36. Van Der Maaten L. 2014 Accelerating t-SNE using tree-based algorithms. *J. Mach. Learn. Res.* **15**, 3221–3245.
37. GBIF.org. 2018 GBIF occurrence downloads, 12 February, 27 February, 27 May, 25 July. See electronic supplementary material, table S2 for list of dois.
38. Hijmans RJ, van Etten J. 2012 raster: Geographic analysis and modeling with raster data. R package version 2.0-12.
39. Becker RA, Wilks AR. 2017 maps: Draw Geographical Maps. R package version 3.2.0. See https://CRAN.R-project.org/package=maps.
40. Wickham H. 2009 *Ggplot2: elegant graphics for data analysis*. New York, NY: Springer.
41. Bischl B, Lang M, Bossek J, Horn D, Richter J, Surmann D. 2017 BBmisc: Miscellaneous Helper Functions for B. Bischl. R package version 1.11.
42. Mouselimis L. 2019 ClusterR: Gaussian Mixture Models, K-Means, Mini-Batch-Kmeans, K-Medoids and Affinity Propagation Clustering. R package version 1.1.8. See https://CRAN.R-project.org/package=ClusterR.
43. Sherratt TN. 2008 The evolution of Müllerian mimicry. *Naturwissenschaften* **95**, 681. (doi:10.1007/s00114-008-0403-y)
44. Paradis E, Schliep K. 2018 ape 5.0: an environment for modern phylogenetics and evolutionary analyses in R. *Bioinformatics* **35**, 526–528. (doi:10.1093/bioinformatics/bty633)
45. Galili T. 2015 dendextend: an R package for visualizing, adjusting, and comparing trees of hierarchical clustering. *Bioinformatics* **31**, 3718–3720. (doi:10.1093/bioinformatics/btv428)
46. Mantel N. 1967 The detection of disease clustering and a generalised regression approach. *Cancer Res.* **27**, 209–220.
47. Dray S, Dufour A. 2007 The ade4 Package: Implementing the duality diagram for ecologists. *J. Stat. Softw.* **22**, 1–20. (doi:10.18637/jss.v022.i04)
48. Arnold JB. 2017 ggthemes: Extra themes, scales and geoms for 'ggplot2.' R package version 3.4. 0.
49. Phillips SJ, Dudík M. 2008 Modeling of species distributions with Maxent: new extensions and a comprehensive evaluation. *Ecography* **31**, 161–175. (doi:10.1111/j.0906-7590.2008.5203.x)
50. Fick SE, Hijmans RJ. 2017 WorldClim 2: New 1-km spatial resolution climate surfaces for global land areas. *Int. J. Climatol.* **37**, 4302–4315.
51. Quantum GIS Development Team. 2018 Quantum GIS Geographic Information System. See www.qgis.org.
52. Huheey JE. 1988 Mathematical models of mimicry. *Am. Nat.* **131**, S22–S41. (doi:10.1086/284765)
53. Rodriguez J, Pitts JP, von Dohlen CD, Wilson JS. 2014 Müllerian mimicry as a result of codivergence between velvet ants and spider wasps. *PLoS ONE* **9**, e112942. (doi:10.1371/journal.pone.0112942)
54. Troscianko J, Stevens M. 2015 Image calibration and analysis toolbox–a free software suite for objectively measuring reflectance, colour and pattern. *Methods Ecol. Evol.* **6**, 1320–1331. (doi:10.1111/2041-210X.12439)
55. Fattig PW. 1933 Food of the robber fly, *Mallophora orcina* (Wied)(Diptera). *Can. Entomol.* **65**, 119–120. (doi:10.4039/Ent65119-5)
56. Bromley SW. 1936 Asilids feeding on bumblebees in New England. *Psyche: J. Entomol.* **43**, 14. (doi:10.1155/1936/95673)
57. Plath OE. 1934 *Bumblebees and their ways*. New York, NY: Macmillan.
58. Morse DH. 1986 Predatory risk to insects foraging at flowers. *Oikos* **46**, 223–228. (doi:10.2307/3565470)
59. Owen JH. 1948 The larder of the red-backed shrike. *British Birds* **41**, 200–203.
60. Davies NB. 1977 Prey selection and the search strategy of the spotted flycatcher (*Muscicapa striata*): a field study on optimal foraging. *Anim. Behav.* **25**, 1016–1033. (doi:10.1016/0003-3472(77)90053-7)
61. Knowlton GF, Maddock DR, Wood SL. 1946 Insect food of the sagebrush swift. *J. Econ. Entomol.* **39**, 382–383. (doi:10.1093/jee/39.3.382)
62. Korschgen LJ, Moyle DL. 1955 Food habits of the bullfrog in central Missouri farm ponds. *Am. Midland Nat.* **54**, 332–341. (doi:10.2307/2422571)
63. Wilson JS, Jahner JP, Williams KA, Forister ML. 2013 Ecological and evolutionary processes drive the origin and maintenance of imperfect mimicry. *PLoS ONE* **8**, e61610. (doi:10.1371/journal.pone.0061610)
64. Beatty CD, Beirinckx K, Sherratt TN. 2004 The evolution of Müllerian mimicry in multispecies communities. *Nature* **431**, 63–66. (doi:10.1038/nature02818)
65. Sherratt TN, Peet-Paré CA. 2017 The perfection of mimicry: an information approach. *Phil. Trans. R. Soc. B* **372**, 20160340. (doi:10.1098/rstb.2016.0340)
66. Ihalainen E, Rowland HM, Speed MP, Ruxton GD, Mappes J. 2012 Prey community structure affects how predators select for Müllerian mimicry. *Proc. R. Soc. B* **279**, 20112360. (doi:10.1098/rspb.2011.2360)
67. Chouteau M, Angers B. 2012 Wright's shifting balance theory and the diversification of aposematic signals. *PLoS ONE* **7**, e34028. (doi:10.1371/journal.pone.0034028)
68. Fisher RA. 1930 *The genetical theory of natural selection*. Oxford, UK: Clarendon Press.
69. Turner JRG. 1975 Communal roosting in relation to warning colour in two heliconiine butterflies (Nymphalidae). *J. Lepidopterists' Soc.* **29**, 221–226.
70. Remington CL. 1968 Suture-zones of hybrid interaction between recently joined biotas. In *Evolutionary biology*, pp. 321–428. Boston, MA: Springer.
71. Swenson NG, Howard DJ. 2005 Clustering of contact zones, hybrid zones, and phylogeographic breaks in North America. *Am. Nat.* **166**, 581–591. (doi:10.1086/491688)
72. Mallet J, Barton NH. 1989 Strong natural selection in a warning-colour hybrid zone. *Evolution* **43**, 421–431. (doi:10.1111/j.1558-5646.1989.tb04237.x)
73. Hewitt G. 2000 The genetic legacy of the Quaternary ice ages. *Nature* **405**, 907–913. (doi:10.1038/35016000)
74. Hewitt GM. 2001 Speciation, hybrid zones and phylogeography—or seeing genes in space and time. *Mol. Ecol.* **10**, 537–549. (doi:10.1046/j.1365-294x.2001.01202.x)
75. Plowright RC, Owen RE. 1980 The evolutionary significance of bumble bee colour patterns: a mimetic interpretation. *Evolution* **34**, 622–637. (doi:10.1111/j.1558-5646.1980.tb04002.x)
76. Blum MJ. 2002 Rapid movement of a Heliconius hybrid zone: evidence for phase III of Wright's shifting balance theory? *Evolution* **56**, 1992–1998. (doi:10.1111/j.0014-3820.2002.tb00125.x)
77. Mallet J. 1986 Hybrid zones of *Heliconius* butterflies in Panama and the stability and movement of warning colour clines. *Heredity* **56**, 191–202. (doi:10.1038/hdy.1986.31)